

Epitaxial aluminium-nitride tunnel barriers grown by nitridation with a plasma source

T. Zijlstra, C. F. J. Lodewijk, N. Vercruyssen, F. D. Tichelaar, D. N. Loudkov, and T. M. Klapwijk,
 Kavli Institute of Nanoscience, Faculty of Applied Sciences, Delft
 University of Technology, Lorentzweg 1, 2628 CJ Delft, The Netherlands

High critical current-density (10 to 420 kA/cm²) superconductor-insulator-superconductor tunnel junctions with aluminium nitride barriers have been realized using a remote nitrogen plasma from an inductively coupled plasma source operated in a pressure range of 10⁻³ to 10⁻¹ mbar. We find a much better reproducibility and control compared to previous work. From the current-voltage characteristics and cross-sectional TEM images it is inferred that, compared to the commonly used AlO_x barriers, the poly-crystalline AlN barriers are much more uniform in transmissivity, leading to a better quality at high critical current-densities.

Quantum technology based on superconducting or magnetic metals uses nanometer thick tunnel barriers. Many routes to quantum computation are based on aluminium with aluminium oxide barriers. Niobium devices use a proximitized layer of aluminium with a similar oxide [1]. Magnetic tunnel junctions have recently moved from using amorphous aluminium oxide to epitaxial magnesium oxide with its unique spin-dependent properties [2, 3]. In quantum computation the amorphous tunnel barrier has surfaced as an important source of decoherence leading to the introduction of an epitaxial aluminium oxide barrier [4, 5]. On the other hand highly transmissive tunnel barriers are urgently needed for sub-millimeter mixers in order to achieve a high bandwidth [6], in electronic refrigeration to maximize the cooling power [7] and in high density magnetic memory devices [8].

It has been demonstrated that a major problem of amorphous AlO_x barriers is that they are laterally inhomogeneous [9, 10]. We take this into account by using a distribution of transparencies T_n by writing for the voltage-independent normal conductance:

$$G \propto \sum_n A_n T_n \quad (1)$$

with A_n a fraction of the total area of the tunnel barrier with an assumed uniform transmissivity T_n . Hence, we do not assume a universal distribution of transparencies [11, 12] but one which is related to a distribution of areas with different transmissivities, resulting from the technological process. For superconducting tunneljunctions (SIS) this amounts to a situation analogous to superconducting quantum point contacts [13]:

$$I \propto \sum_n A_n j(V, T_n) \quad (2)$$

with I the total current and $j(V, T_n)$ the voltage-dependent current-density per area A_n . j contains contributions of different orders proportional to T_n , T_n^2 , T_n^3 , etcetera, reflecting multiple Andreev reflections ($j(V, T_n) = j_1(V, T_n) + j_2(V, T_n^2) + j_3(V, T_n^3) + \dots$). For the commonly used low current-density tunnelbarriers

most A_n have T_n of the order of 10⁻⁴. Since for SIS junctions first order tunneling j_1 leads to a zero subgap current, the remaining subgap current is due to the higher order terms (j_2, j_3, \dots), which only appear for $T_n \approx 1$. Non-uniformity, causing the emergence of areas with $T_n \approx 1$, thus leads to excessive subgap currents. Therefore the critical current density of amorphous aluminium oxide barriers is limited to 20 kA/cm² [14]. We will demonstrate that aluminium nitride barriers are superior to aluminium oxide barriers with respect to barrier uniformity.

In the work reported here a very good reproducibility is realized by using the afterglow region of a nitrogen plasma from an inductively coupled plasma source (CO-PRA) (see for example Weiler [15]), from CCR technology. The plasma provides the energy to split the N₂ molecules into N radicals, needed for the growth of AlN. The source is mounted on a vacuum chamber. The plasma is created in the source and diffuses into the chamber. We have chosen to work in a range of high pressures (2 × 10⁻³ mbar to 1 × 10⁻¹ mbar), for two reasons. First, we expect at these higher pressures a larger fraction of atomic N. Secondly, the ion energies in this regime are as low as a few eV, which minimizes damage to the barrier-formation. This is different from recent work, where the plasma process not only provides the chemically active species but also creates damage by highly energetic ions [16, 17, 18, 19, 20] (although usable routes have been reported [18]). In addition many other plasma techniques suffer from instabilities, resulting in a poor process reproducibility.

The devices are fabricated on a 2 inch oxidized silicon or fused quartz substrate. All metal layers are deposited by magnetron sputtering in the process chamber of a Kurt Lesker system. First, a 100 nm Nb monitor layer is deposited, after which a ground plane pattern is optically defined. Subsequently, a bilayer of 100 nm Nb and about 7 nm Al is deposited. Without breaking the vacuum, the substrate is then transferred to a nitridation chamber, where the Al is exposed to the nitrogen plasma for several minutes, producing a layer of AlN. The substrate is then again *in vacuo* transferred to the

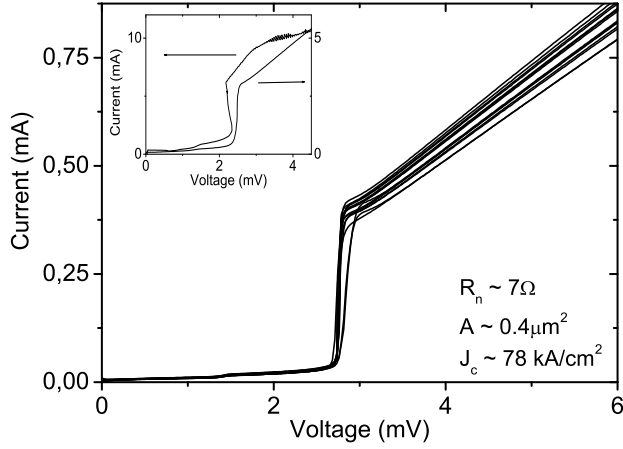


FIG. 1: Current-voltage characteristics of a typical batch of Nb/AlN/Nb junctions. Junction area is about $0.4 \mu\text{m}^2$, for a normal resistance, R_n , of 6.8Ω (critical current density $\sim 78 \text{ kA/cm}^2$). The Josephson current has been suppressed with a magnetic field. Inset shows IV characteristics of SIS junctions with J_c of 130 kA/cm^2 and 420 kA/cm^2 . For the latter thermal heating causes gap-suppression and back-bending.

process chamber, where a top electrode of 200 nm Nb is deposited. The lateral dimensions of the multilayer of Nb/Al/AlN/Nb are patterned by lift-off. Junctions are defined by e-beam lithography with a negative e-beam resist (SAL-601) layer and reactively ion etched (RIE) with a SF_6/O_2 plasma using the AlN as an etch-stop, followed by a mild anodization (5 V). The junction resist pattern is used as a self-aligned lift off mask for a dielectric layer of 250 nm SiO_2 . A 500 nm Nb/ 50 nm Au top layer is deposited and Au is etched with a wet etch in a KI/I_2 solution using an optically defined mask. Finally, using an e-beam defined top wire mask pattern, the layer of Nb is etched with a SF_6/O_2 RIE, which finishes the fabrication process.

The fabrication process used provides a very good reproducibility. There is reproducibility within one fabrication run, illustrated by the similarity of junctions on a produced wafer. Scatter in the normal resistance R_n of the junctions is caused by variation in the junction area A , due to uncertainties in junction definition, and variation in the barrier-specific $R_n A$ value. For 34 junctions, of which 14 are shown in Fig. 1, the standard deviation, $\sqrt{\sum_{i=1}^m (R_{n,i} - \langle R_n \rangle)^2 / (m - 1)}$, with m the number of junctions, of R_n has been determined to be 3.3% relative to the average, $\langle R_n \rangle = 6.8 \Omega$. The peak-to-peak variation amounts to $\pm 6 \%$. By measuring four big junctions (two of $1 \mu\text{m}^2$ and two of $2 \mu\text{m}^2$), the value of $R_n A$ has been found to be $2.8 \Omega\mu\text{m}^2$ (corresponding to a critical current density $J_c \approx 78 \text{ kA/cm}^2$). Assuming perfect junction definition (which is most likely not the case), the standard deviation of $R_n A$ within one fabrication run is at most 3.3% . Based on the average R_n , A is $0.4 \mu\text{m}^2$.

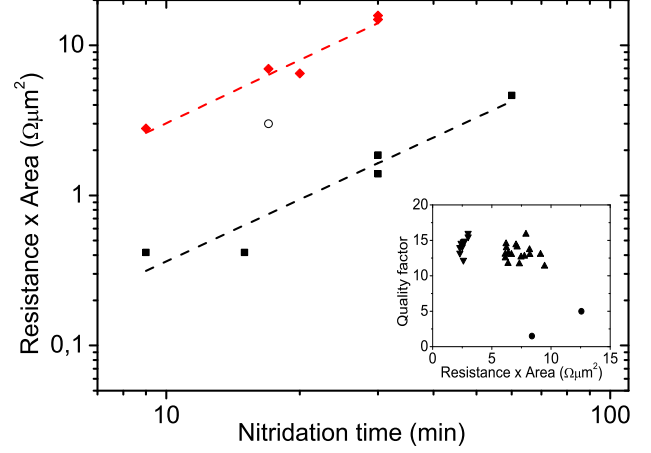


FIG. 2: $R_n A$ product as a function of nitridation time, t_N , for nine different fabricated batches. The squares represent data for a 30 cm chuck-source distance, whereas the diamonds indicate a 15 cm chuck-source distance. The open circle represents the junctions of Fig. 1. Dashed lines indicate both a dependence $R_n A \propto t_N^{1.4}$. Inset: Quality factor as a function of $R_n A$ product for two batches of Nb/AlN/Nb junctions (up- and down-pointing triangles). Also indicated are AlO_x data from Miller *et al.* [14] (filled circles).

We also find a good reproducibility from run to run. We have made several batches, varying the nitridation time t_N from 9 to 60 minutes. About half of the batches has been made with a low position of the chuck (30 cm distance to the plasma source) in the nitridation chamber, the other half with a higher position (15 cm distance to the plasma source). In Fig. 2, we plot the $R_n A$ product of the batches as a function of t_N for the large chuck-source distance (squares) and for the small chuck-source distance (diamonds). The dashed lines indicate a dependence $R_n A \propto t_N^k$, with $k = 1.4$. Obviously, there is a systematic dependence on nitridation time, indicating a well-behaving process. By varying the nitridation time and/or the chuck position, we can realize any desired $R_n A$ value between $0.5 \Omega\mu\text{m}^2$ and $10 \Omega\mu\text{m}^2$.

The quality factor Q , defined as R_{sg}/R_n , where R_{sg} is the subgap resistance, gives an indication of the subgap leakage through the tunnel barrier. In the inset of Fig. 2, Q has been plotted for two different batches of AlN based junctions, together with data on AlO_x from Miller *et al.* [14]. In contrast to these AlO_x devices, it is evident that Q is higher than 10 for all AlN devices. The lower subgap currents prove that our AlN barriers have a lower density of areas with $T_n \approx 1$, in other words a better uniformity.

As shown in Fig. 2, we reach $R_n A$ products as low as $0.4 \Omega\mu\text{m}^2$, corresponding to a J_c of 420 kA/cm^2 . For such high current densities, heating effects decrease the superconducting gap voltage of the junction in the form of back-bending (Fig. 1 Inset). Up to at least 130 kA/cm^2 , this effect remains hidden, but is still present. This in-

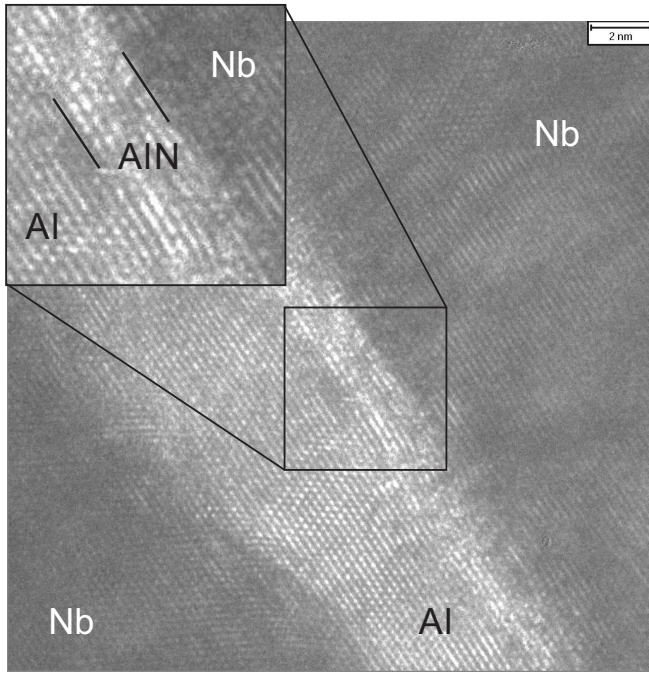


FIG. 3: High resolution transmission electron microscope (HRTEM) micrographs of an AlN dielectric barrier deposited on an Al layer (bright region) between Nb electrodes (dark regions). The bar in the top-right corner represents a length of 2 nm.

indicates that for these AlN barriers the maximum critical current density is no longer limited by the materials control of the barrier, but by the intrinsic physical process of nonequilibrium in the electrodes. Consequently, a future detailed statistical evaluation of reproducibility and control has to take into account the distortions of the IV curves by heating.

Using high-resolution transmission electron microscopy (HRTEM) we find that the AlN-barrier is grown epitaxially (Fig. 3). The barrier is visible as a region with higher transmission (most bright region) and in a small difference in lattice spacing for Al and AlN. The images clearly indicate epitaxial alignment of the crystalline structure of the AlN with the underlying Al crystal. The lattice plane distances of the planes parallel to the surface were measured in various locations and identified as either $\{0002\}$ or $\{1\bar{1}01\}$ planes in the hexagonal AlN phase, with spacing $2.49 \pm 0.06 \text{ \AA}$ and $2.37 \pm 0.06 \text{ \AA}$ respectively. An averaged thickness of the barrier of about $1.5 \pm 0.5 \text{ nm}$ is found. For these devices the $R_n A$ value is about $16 \Omega \mu\text{m}^2$. Obviously, in contrast to the commonly used AlO_x , the AlN tunnel barrier has a crystalline nature with a thickness of about 6 lattice planes, which may be the cause of the better uniformity.

In conclusion, epitaxial aluminium-nitride tunnel barriers have been grown, at ambient temperature, using a plasma-source to generate chemically active nitrogen.

This method shows significantly better reproducibility than other AlN growth techniques have shown in the past. Compared to the conventionally used aluminium oxide barriers, much better quality current-voltage characteristics are observed for high critical current densities, which is attributed to a spatially more uniform transmissivity of the epitaxial tunnel barrier.

The authors would like to thank B. de Lange for technical assistance, and P. C. Snijders and R. W. Simmonds for discussions. We thank NanoImpuls, Nanofridge, the Dutch Research School for Astronomy (NOVA), the Dutch Organisation for Scientific Research (NWO), and the European Southern Observatory (ESO) for funding this project.

-
- [1] M. Gurvitch, M. A. Washington, and H. A. Huggins, *Appl. Phys. Lett.* **42**, 472 (1983).
 - [2] S. S. P. Parkin, *et al.*, *Nature Materials* **3**, 862 (2004).
 - [3] S. Yuasa, T. Nagahama, A. Fukushima, Y. Suzuki, and K. Ando, *Nature Materials* **3**, 868 (2004).
 - [4] S. Oh, *et al.*, *Supercond. Sci. Technol.* **18**, 1396 (2005).
 - [5] S. Oh, K. Cicak, J. S. Kline, M. A. Sillanpää, K. D. Osborn, J. D. Whittaker, R. W. Simmonds, and D. P. Pappas, *Phys. Rev. B* **74**, 100502(R) (2006).
 - [6] J. Kawamura, D. Miller, J. Chen, J. Zmuidzinas, B. Bumble, H. G. LeDuc, and J. A. Stern, *Appl. Phys. Lett.* **76**, 2119 (2000).
 - [7] F. Giazotto, T. T. Heikkilä, A. Luukanen, A. M. Savin, J. P. Pekola, *Rev. Mod. Phys.* **78**, 217 (2006).
 - [8] K. Tsunekawa, *et al.*, *IEEE Trans. Magn.* **42**, 103 (2006).
 - [9] W. H. Rippard, A. C. Perrella, F. J. Albert, and R. A. Buhrman, *Phys. Rev. Lett.* **88**, 046805 (2002).
 - [10] K. M. Lang, D. A. Hite, R. W. Simmonds, R. McDermott, D. P. Pappas, and J. M. Martinis, *Rev. Sci. Instr.* **75**, 2726 (2004).
 - [11] K. M. Schep, and G. E. W. Bauer, *Phys. Rev. Lett.* **78**, 3015 (1997).
 - [12] Y. Naveh, V. Patel, D. V. Averin, K. K. Likharev, and J. E. Lukens, *Phys. Rev. Lett.* **85**, 5404 (2000).
 - [13] E. Scheer, P. Joyez, D. Esteve, C. Urbina, and M. H. Devoret, *Phys. Rev. Lett.* **78**, 3535 (1997).
 - [14] R. E. Miller, W. H. Mallison, A. W. Kleinsasser, K. A. Delin, and E. M. Macedo, *Appl. Phys. Lett.* **63**, 1423 (1993).
 - [15] M. Weiler, K. Lang, E. Li, J. Robertson, *Appl. Phys. Lett.* **72**, 1314 (1998).
 - [16] T. Shiota, T. Imamura and S. Hasuo, *Appl. Phys. Lett.* **61**, 1228 (1992).
 - [17] Z. Wang, A. Kawakami, and Y. Uzawa, *Appl. Phys. Lett.* **70**, 114 (1997).
 - [18] B. Bumble, H. G. LeDuc, J. A. Stern and K.G. Megerian, *IEEE Trans. Appl. Superconduct.* **11**, 76 (2001).
 - [19] A. B. Kaul, A. W. Kleinsasser, B. Bumble, H. G. LeDuc and K. A. Lee, *J. Mater. Res.* **20**, 3047 (2005).
 - [20] N. N. Iosad, A. B. Ermakov, F. E. Meijer, B. D. Jackson, and T. M. Klapwijk, *Supercond. Sci. Technol.* **15**, 945 (2002).